Computational modeling of pharmacokinetics and tumor dynamics to guide anti-cancer treatment

Yin, A.

Chapter 7

Population pharmacokinetic and toxicity analysis of high-dose methotrexate in patients with central nervous system lymphoma

Anyue Yin, Fleur A. de Groot, Henk-Jan Guchelaar, Marcel Nijland, Jeanette K. Doorduijn, Daan J. Touw, Thijs Oude Munnink, Brenda C.M. de Winter, Lena E. Friberg, Joost S.P. Vermaat, Dirk Jan A.R. Moes

In preparation

Abstract

Background: High-dose methotrexate (HD-MTX) based polychemotherapy is widely used for patients with central nervous system (CNS) lymphoma. The pharmacokinetic (PK) variability and unpredictable occurrence of toxicity remain major concerns in HD-MTX treatment.

Objectives: This study aimed to characterize the population PK of HD-MTX in patients with CNS lymphoma and to identify baseline predictors and exposure thresholds that predict a high risk of renal and hepatotoxicity.

Methods: Routinely monitored serum MTX concentrations after intravenous infusion of HD-MTX and MTX dosing information were collected retrospectively. Acute event of toxicity was defined according to the Common Terminology Criteria for Adverse Events (CTCAE) version 5.0. A population PK model was developed in NONMEM. Toxicity data were analyzed using a logistic regression model and potential baseline and exposure-related predictors were investigated.

Results: In total 1584 MTX concentrations from 110 patients were available for the analysis. A two-compartment population PK model adequately described the data. Estimated glomerular filtration rate (eGFR), treatment regimen, albumin, alkaline phosphatase, and body weight were identified as significant covariates that explain PK variability of HD-MTX. Baseline eGFR and sex were identified as significant predictors for renal toxicity, and MTX dose (mg/m^2) was the strongest predictor for hepatotoxicity. The MTX area under the concentration-time curve ($AUC_{24-\infty}$) and concentration at 24 hours (C_{24h}) showed to correlate with renal toxicity only, and $AUC_{24-\infty} > 109.5$ μmol/L*h and $C_{24h} > 8.64$ μmol/L were potential exposure thresholds predicting a high risk.

Conclusion: A population PK model was developed for HD-MTX in patients with CNS lymphoma. The toxicity analysis showed that low baseline eGFR and male sex, and high MTX dose are associated with increased risk of acute renal and hepatotoxicity, respectively. $AUC_{24-\infty} > 109.5$ μmol/L*h and $C_{24h} > 8.64$ μmol/L were potential exposure thresholds predicting a high risk of renal toxicity. The models hold the potential to guide HD-MTX dosage individualization and better prevent acute toxicity.

1. Introduction

High-dose methotrexate (HD-MTX)-based polychemotherapy is the standard therapy for patients with primary central nervous system (CNS) lymphoma [1, 2]. It is also widely used for patients with secondary CNS involvement of diffuse large B-cell lymphoma (DLBCL), mainly for those who are naive for HD-MTX [3].

The standard dose of HD-MTX for patients with CNS lymphoma is 3 g/m^2 and is administrated by intravenous infusion. Methotrexate (MTX) has approximately 50% protein binding and is eliminated primarily unchanged by renal excretion (> 80%) while a small fraction is eliminated as an metabolite 7-hydroxymethotrexate [4, 5].

In routine HD-MTX treatment, MTX concentrations are monitored after each administration until they reach a safe target (< 0.2 μM). Although HD-MTX dose is based on patients' body surface area (BSA), significant inter- and intra-individual variability in its pharmacokinetics (PK) is observed [6-8]. Delayed elimination of MTX due to impaired renal function or extravascular fluid collections can occur which will result in a prolonged period of MTX exposure and a higher risk of toxicity [4, 7, 8]. Furthermore, the unpredictable occurrence of acute toxicity during HD-MTX treatment, including kidney dysfunction and hepatotoxicity, may result in treatment interruption or delay which could cause unfavorable treatment outcome [6, 7]. To improve the outcomes of HD-MTX therapy, further individualizing HD-MTX dosage and identifying factors that predict a high risk of HD-MTX induced toxicity are desired.

The risk factors that have been identified for HD-MTX induced renal toxicity in patients with lymphoid or hematological malignancy are mostly dose- or exposure-related: doses ≥ 6 g/m^2, area under the concentration-time curve (AUC) in the first administration cycle, and dose-normalized concentration at 24 and 48 hours [9-11]. For HD-MTX induced hepatotoxicity, studies on risk factors are limited but one study suggested that AUC of HD-MTX is associated with hepatotoxicity [12]. Yet, an exposure threshold for toxicity which would facilitate better supportive care and treatment individualization for HD-MTX is still missing. Moreover, the predictors at baseline for HD-MTX induced toxicities are less studied. One study showed that baseline lactate dehydrogenase and albumin correlated with the risk of acute kidney injury [13]. Further exploration of potential risk factors at baseline for both renal and hepatotoxicity would therefore be beneficial to guide HD-MTX therapy.

Population PK-pharmacodynamic (PD) modeling with mixed-effect models enables to quantitatively characterize as well as predict drug PK, response, or toxicity profiles and their relationships in both population and individual levels. This approach also enables

identification of covariates that explain the observed inter- and intra-individual variabilities [14]. Combined with simulations, the developed model can be applied to guide treatment rationally [15]. Until now, several population PK models of HD-MTX in patients with lymphoid malignancy have been published but many were not specifically focused on patients with CNS lymphoma [8, 10, 12, 16-21]. Subsequent toxicity analysis of HD-MTX for patients with CNS lymphoma with a model-based approach is still lacking.

In the current study, based on retrospectively collected data, we performed a population PK analysis to characterize HD-MTX PK in patients with CNS lymphoma who received various treatment regimens, and explored covariates that explain the variability. Subsequently, the occurrence of acute renal and hepatotoxicity were analyzed with a model-based approach which aims to identify baseline predictors and exposure threshold that predict a high risk of toxicity for each HD-MTX administration cycle.

2. Method

2.1 Patients and data

Patients who were diagnosed with CNS lymphoma, treated with HD-MTX based polychemotherapy with available dosing information and MTX concentrations in the period ranging from 2010 to March 2021 from the Leiden University Medical Center (LUMC), Erasmus Medical Center (EMC), and University Medical Center Groningen (UMCG) were included. Patients received HD-MTX by intravenous infusion and were dosed per body surface area (BSA). All medications that have potential drug-drug interaction with MTX (e.g. benzimidazoles and nonsteroidal anti-inflammatory drugs (NSAIDs)) were stopped 72 hours prior to the use of HD-MTX.

The routinely monitored MTX concentrations were retrospectively collected from the laboratory information system (LIS). MTX concentrations were analyzed with ARK™ assay [22] with a lower limit of quantification (LLOQ) of 18.2 μg/L (0.04 μmol/L) in the LUMC and the EMC and 15 μg/L in the UMCG. If the detected MTX was above 50 μmol/L at 24 hours, or above 5 μmol/L at 48 hours, or above 0.2 μmol/L at 72 hours after administration of HD-MTX, it was defined as delayed elimination [4]. Patients' demographic characteristics, drug dosing information (i.e. treatment regimen, infusion hours, and dose), and laboratory results (i.e. serum creatinine (SCr), alkaline phosphatase (ALP), aspartate aminotransferase (ASAT), alanine aminotransferase (ALAT), albumin, bilirubin) were collected from patients' electronic health care records. Based on the available data, estimated glomerular filtration rate (eGFR) was also estimated with the CKD-EPI creatinine equation and included in the analysis [23].

This study is approved by the local Ethical Committee of each institute (number G20.126), and did not fall within the scope of the WMO (Medical Scientific Research Act). A waiver for informed consent was granted. All performed procedures were in accordance with the ethical standards of the institutional medical ethical committee and the 1964 Declaration of Helsinki and its later amendments.

2.2 Population PK modeling

A population PK model was developed based on the available MTX PK data. The unit of MTX concentrations was unified to μg/L by multiplying the data reported in μmol/L by the molar mass of MTX (454.44 g/mol). The data that were below LLOQ were omitted from the analysis due to the small proportion (< 10%) [24].

One-, two- and three-compartment models with first-order elimination were explored as the structural model. Parameters were assumed to be log-normally distributed and inter-individual variability (IIV) was quantified. Inter-occasion variability (IOV) was incorporated on the PK parameter clearance (CL) to account for the intra-individual variability, and each administration cycle was defined as an occasion. A combined proportional and additive error model was applied to characterize the residual errors. The residual errors of data from different medical centers were set to follow the same distribution. The structural model was selected based on goodness-of-fit (GOF), objective function value (OFV) and the stability of the model.

Subsequently, the covariate effects of patients' demographic information, treatment regimen, time-varying laboratory results on CL, and body size related characteristics on volumes of distribution were investigated. The stepwise covariate modelling (SCM) function was applied with assistance of Perl-speaks NONMEM (version 4.9) [25]. Model selection was based on a reduction in OFV assuming a χ^2 distribution, a reduction in IIV or IOV, and physiological plausibility. Both a forward inclusion ($p < 0.05$, $\Delta OFV < -3.84$, degrees freedom = 1) and a backward elimination process ($p < 0.01$, $\Delta OFV > 6.64$, degrees freedom = 1) were performed to identify significant covariates.

2.3 Toxicity analysis

At each HD-MTX administration cycle, the renal and hepatotoxicity were graded based on monitored SCr and ALAT results according to the NCI Common Terminology Criteria for Adverse Events (CTCAE) version 5.0, respectively [26]. The ≥ grade 1 toxicity was defined as a toxicity event. The data were analyzed with a logistic regression model where the probability of having toxicity was estimated. The logit function is shown in Eqs. 7.1–7.3,

where *base* represents baseline logit score, θ is the typical population probability operator, η_i represents the random IIV which was assumed to be normally distributed with mean of 0 and variance of ω2.

Individual PK parameters obtained from the final PK model were applied to simulate and estimate the MTX exposure metrics of interest: AUC between 24 hours after drug administration to infinity ($AUC_{24-\infty}$) and MTX concentration at 24 hours (C_{24h}). The $AUC_{24-\infty}$ were estimated by integrating the individual concentration-time curves from 24 hours to last sample time plus AUC from the last sample time to infinity which was approximated as last concentration divided by terminal elimination rate constant (β).

The baseline predictors and exposure-related predictors were investigated by being included linearly into the logit function (Eq. 7.4). The evaluated baseline factors include patients' demographic information, baseline eGFR, ALAT, ASAT, and albumin of each administration cycle, dose amount, treatment regimen, dose divided by baseline CL as an AUC approximation (AUC_{base}) of each administration cycle, $AUC_{24-\infty}$ from previous administration course ($pAUC_{24-\infty}$), and C_{24h} from previous administration course (pC_{24h}). The toxicity status in the previous administration course was also evaluated as a potential predictive factor. The inclusion of covariates was based on the reduction in OFV and physiological plausibility. A forward inclusion process was performed when investigating baseline predictors. Factors that result in a ΔOFV < -3.84 were considered to be significant ($p < 0.05$, degrees freedom = 1).

$$base = \ln\left(\frac{\theta}{1-\theta}\right) \quad \text{Eq. 7.1}$$

$$logit_i = base + \sum_{k=1}^{n} E_{cov\_k} + \eta_i \quad \text{Eq. 7.2}$$

$$P_i = \frac{e^{logit_i}}{1 - e^{logit_i}} \quad \text{Eq. 7.3}$$

$$E_{cov\_k} = \begin{cases} categorical: \theta_{cov} \\ continuous: \left(\frac{COV}{median(COV)}\right)^{\theta_{cov}} \end{cases} \quad \text{Eq. 7.4}$$

2.4 Model evaluation

The final PK model was evaluated with GOF plots, prediction-corrected visual predictive check (pcVPC), and a bootstrap based on 1000 runs of replicated datasets sampled from original dataset with replacement.

The pcVPC plot was generated based on 1000 times of simulation. MTX concentrations were commonly monitored at 24 hours, 48 hours, and 72 hours, and thereafter every 24 hours after the start of infusion until the concentration was below a threshold. Consequently, patients with delayed elimination had a longer follow-up and more samples per patient. The same sampling strategy was applied when performing simulations for the pcVPC plot, i.e., if the simulated concentration after day 3 fell below 0.1 μmol/L, the next data point would not be sampled. The set threshold of 0.1 μmol/L is the median of the second last monitored concentration of the collected data after day 3.

The adequacy of the toxicity model was evaluated with a visual predictive check (VPC). The original dataset was simulated 500 times to derive the 90% prediction interval of the proportion of patients having toxicity at each administration cycle and over a range of covariate values. The prediction interval was compared with the observed results.

2.5 Software and estimation method

The population modelling analysis was performed with NONMEM (version 7.4.4, ICON Development Solutions, Ellicott City, MD, USA) aided with Perl-speaks-NONMEM (PsN) (version 4.9, Uppsala University, Uppsala, Sweden) [27]. Parameters of the population PK model were estimated using the first order conditional estimation method with interaction (FOCEI). Conditional Laplacian method was used to approximate the marginal likelihood in the toxicity analysis. Data management and plots generation were performed with R statistics software (version 4.2.1, R Foundation for Statistical Computing, Vienna, Austria).

3. Results

3.1 Patients and PK data

In total 110 patients with CNS lymphoma (56 males and 54 females) were included from the LUMC (n = 75), the UMCG (n = 17), and the EMC (n = 18). Among the included patients, 80 patients (73%) were diagnosed with primary CNS lymphoma, 11 patients (10%) were diagnosed with secondary CNS lymphoma, and 11 patients (10%) had secondary CNS involvement of systemic DLBCL. The baseline characteristics of the included patients from 3 medical centers are shown in **Table 7.1**.

In total, 1584 monitored MTX concentrations from 412 administration cycles were collected, of which 124 (7.8%) were below the LLOQ and were omitted from the analysis.

Table 7.1: Baseline characteristics of the patients included in the current study

Item	N (%) / Median (Range)		
Center	LUMC	UMCG	EMC
Number of patients	75	17	18
Age (year)	66 (22–83)	66 (52–73)	67 (51–76)
Sex			
Male	42 (56%)	6 (35%)	8 (44%)
Female	33 (44%)	11 (65%)	10 (56%)
Body weight (kg)	78 (53.4–115)	76.5 (46.4–108)	70.1 (49.5–96.3)
Height (cm)	176 (155–195)	169 (158–192)	168 (148–186)
Body mass index (kg/m^2)	25.0 (17.6–38.0)	25.0 (17.9–35.4)	23.7 (18.9–34.5)
Body surface area (m^2)	1.94 (1.58–2.34)	1.94 (1.44–2.40)	1.8 (1.41–2.05)
ASAT (IU/L)	20 (9–100)	20.3 (10–53)	22.5 (14–58)
ALAT (IU/L)	30.5 (9–286)	43 (16–213)	41 (13–215)
SCr (μmol/L)	64 (37–125)	66 (43–94)	65 (45–98)
eGFR (ml/(min*1.73 m^2)) [a]	93.8 (52.9–159)	89.3 (54–113)	90.3 (66.9–115)
Albumin (g/L)	38.5 (28–49)	37.5 (32.5–45.4)	40 (34–49)
ALP (U/L)	67 (25–297)	60 (44–82)	62.5 (28–118)
Bilirubin (μmol/L)	8 (3–23)	7.7 (3–25.3)	8 (4–19)
Disease type			
PCNSL	45 (60%)	17 (100%)	18 (100%)
SCNSL	11 (14.7%)	0	0
Stage IV DLBCL with CNS involvement	11 (14.7%)	0	0
Other lymphoma with CNS involvement [b]	8 (10.7%)	0	0
Number of administration cycles per patient	4 (1–8)	4 (3–4)	4 (1–8)
Dose of MTX (mg/m^2)	3000 (1500–8000)	3000 (1950–3000)	3000 (1500–3200)
Treatment regimens [c]			
RMP	35 (46.7%)	0	0
MATRIX	40 (53.3%)	0	0
MBVP	0	17 (100%)	18 (100%)

ALAT, alanine aminotransferase; ALP, alkaline phosphatase; ASAT, aspartate aminotransferase; CNS, central nervous system; DLBCL, diffuse large B-cell lymphoma; eGFR, estimated glomerular filtration rate; MTX, methotrexate; PCNSL, primary CNS lymphoma; SCNSL, secondary CNS lymphoma; SCr, serum creatinine.
[a] eGFR was estimated with the CKD-EPI creatinine equation.
[b] Including T cell lymphoma, Follicular lymphoma, and Burkitt lymphoma
[c] RMP, contains high-dose MTX (HD-MTX), rituximab and procarbazine; MATRIX, contains HD-MTX, high-dose cytarabine (HD-AraC), thiotepa, and rituximab; MBVP, contains HD-MTX, teniposide, carmustine, prednisolone, with or without rituximab or HD-AraC. Details can be found in Online Resource, Table S7.1.

The concentrations were monitored daily after the start of MTX infusion until the concentrations fell to a level below 0.2 μmol/L or the LLOQ. The median number of concentrations contributed by each patient to the analysis was 12, ranging from 2 to 35. The delayed elimination was observed in 47 (31.3%) patients and the longest follow-up time during one administration cycle was 454 hours. Five patients had a treatment interruption of more

than 2.5 months and their data before and after the interruption were treated as data from two separate subjects. This resulted in 115 subjects in the dataset eventually. The time-course of all collected MTX concentrations is shown in **Online Resource 7.1**, **Figure S7.1**.

The treatment regimen differs among medical centers (**Table 7.1**, **Online Resource 7.1**, **Table S7.1**). The LUMC patients were separated into 2 treatment groups. Older and/or less fit patients received HD-MTX with rituximab and procarbazine (RMP). For younger and fit patients (< 70 years old), HD-MTX was given with high-dose cytarabine (HD-AraC), thiotepa, and rituximab (MATRIX). As for the UMCG and the EMC patients, HD-MTX was administered with teniposide, carmustine, prednisolone, with or without rituximab or HD-AraC (MBVP). Details about the treatment regimens including infusion durations can be found in **Online Resource 7.1**, **Table S7.1**.

3.2 Population PK model

A two-compartment population PK model with first-order elimination provided the best fit to the obtained data in HD-MTX in patients with CNS lymphoma. Compared with the one-compartment model, the objective function value (OFV) of the two-compartment model was 1843.772 units lower ($p < 0.01$, degree of freedom = 4). Although the three-compartment model showed to further improve the model fit, the estimated relative standard errors (RSEs) of parameters indicated unreliable parameter estimates. Therefore, the two-compartment model was selected as the structural model.

The covariate analysis identified eGFR, treatment regimen, albumin, and ALP are significant covariates on CL of MTX ($p < 0.01$). Body weight was a significant covariate on the volume of distribution of the central compartment (V1). The RSEs indicate an acceptable precision (< 40%) of most parameters except for the coefficient of ALP effect (**Table 7.2**). The typical MTX CL in patients in the RMP group was estimated to be 16.0 % lower than that in the MATRIX group, while the CL differences between the MATRIX and MBVP groups were not significant (**Table 7.2**, **Online Resource 7.1**, **Figure S7.2**). The coefficient of variation (CV%) of random IIV and IOV for CL decreased from 29.2% and 23.1% to 15.5% and 12.3%, respectively, after covariate inclusions. The inclusion of IIV on V_1 became insignificant after covariate inclusions and was therefore fixed to zero (OFV increased by 2.265). The estimated standard deviation (SD) of the additive residual error approached zero and was therefore fixed to 0.0001 μg/L.

The GOF plots in both normal and logarithmic scale showed that the model predictions were generally in good accordance with the observations, while the population predictions underpredicted the observations at lower concentrations (**Figure 7.1**). The deviations

between model predictions and observations were also observed when the concentrations were above 20,000 µg/L. However, when it was explored to remove these data points, the new parameter estimates were still within the estimated 95% confidence interval (CI) of the current parameter estimates. The conditional weighted residual errors (CWRES) were distributed around zero without obvious trends over time, but trends over population predictions at lower concentrations can be observed (**Figure 7.1**). The pcVPC plot demonstrated an adequate predictability of the model (**Figure 7.2**). The final parameter estimates were in good agreement with the bootstrap results (**Table 7.2**).

Table 7.2: Parameter estimates of the final population PK model of HD-MTX in patients with CNS lymphoma

				Bootstrap	
	Estimate (RSE)	IIV (CV%) (RSE%) [shrinkage]	IOV (CV%) (RSE%)	Median	95% CI
CL (L/h)	21.2 (13%)	15.5 (8%) [10%]	12.3 (6%)	21.4	[17.2, 27.2]
θ_{eGFR}	0.0104 (5%)	-		0.0104	[0.0093, 0.011]
θ_{TREAT}					
MATRIX	1	-		-	-
RMP	0.840 (4%)	-		0.839	[0.772, 0.913]
MBVP	1.03 (3%)	-		1.03	[0.952, 1.11]
θ_{ALB}	0.225 (28%)	-		0.225	[0.0715, 0.369]
θ_{ALP}	-0.0624 (41%)	-		-0.0656	[-0.115, -0.0186]
V_1 (L)	125 (16%)	0 FIX		126.4	[98.1, 172]
θ_{WT}	0.00370 (34%)	-		0.00369	[0.00127, 0.00629]
V_2 (L)	36.7 (27%)	55.7 (11%) [13%]		38.1	[23.9, 62.4]
Q (L/h)	0.593 (21%)	30.2 (15%) [15%]		0.605	[0.418 0.920]
Residual errors					
Prop. (CV%)	25.2% (4%)	[18%][a]		25.0%	[23.0%, 26.9%]
Add. (SD, µg/L)	0.0001 FIX	-		0.0001 FIX	-

Add., additive residual error; ALB, albumin; ALP, alkaline phosphatase; CI, confidence interval; CL, clearance; CV, coefficient of variation; eGFR, estimated glomerular filtration rate; IIV, inter-individual variability; IOV, inter-occasion variability; Prop., proportional residual error; Q, distribution clearance; RSE, relative standard error; SD, standard deviation; V1, distribution volume of the central compartment; V2, distribution volume of the peripheral compartment; WT, weight; MATRIX, RMP, and MBVP, three different treatment regimens.

[a] Epsilon shrinkage.

$$V_{1i} = 125 * \left(1 + \theta_{WT} * (WT - 75.8)\right) * e^{\eta_i}$$

$$CL_i = 21.2 * \left(1 + \theta_{eGFR} * (eGFR - 82.93)\right) * \left(\frac{ALB}{37.31}\right)^{\theta_{ALB}} * \left(\frac{ALP}{73.81}\right)^{\theta_{ALP}} * \theta_{TREAT} * e^{\eta_i}$$

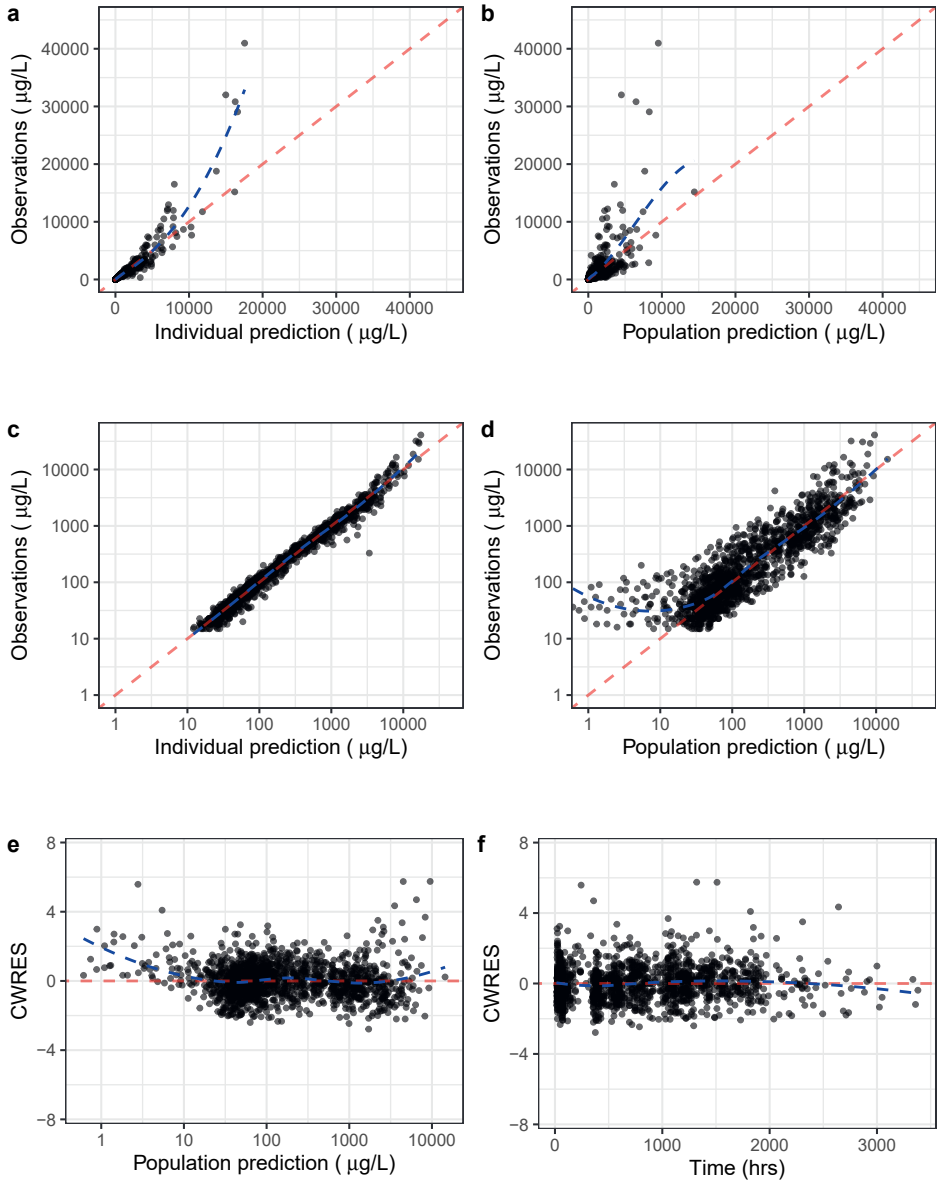

Figure 7.1: Goodness-of-fit plots of the developed population PK model, including observations versus individual predictions in both normal (a) and logarithmic scale (c), observations versus population predictions in both normal (b) and logarithmic scale (d), and conditional weighted residual errors (CWRES) versus populations predictions (e) and time after last dose (f). The red dashed lines represent y = x (a, b, c, d) and y = 0 (e, f). Black dashed lines represent corresponding loess regressions.

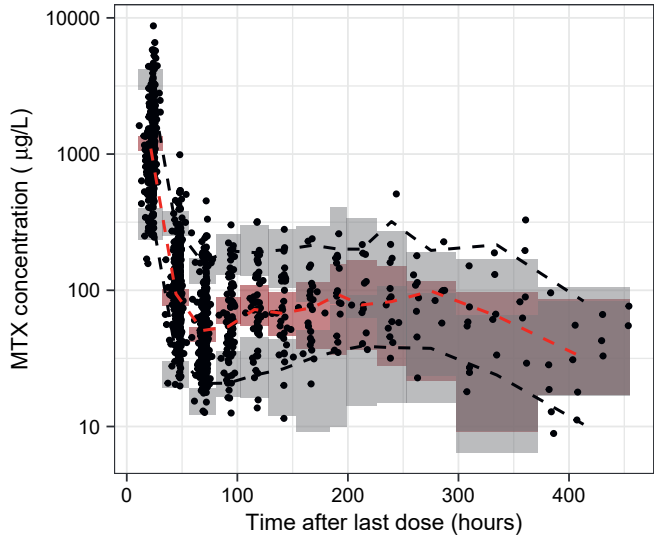

Figure 7.2: Prediction-corrected visual predictive check (pcVPC) of the final HD-MTX pharmacokinetic model. Black points represent observations, black dashed lines represent 95th and 5th percentile of the observations, red dashed line represents the 50th percentile of the observations, grey shaded areas represent 95% confidence interval of the 95th and 5th percentiles of the simulations, and red shaded area represents 95% confidence interval of the 50th percentile of the simulations.

3.3 Toxicity analysis

Among the 115 subjects, 51 (44.3%) and 76 (66.1%) subjects developed acute renal and hepatotoxicity during at least one administration cycle, respectively. The majority of subjects received ≤ 4 courses of treatment (98/115, 85.2%). The observed proportion of patients having each grade of renal or hepatotoxicity during each administration cycle were shown in **Online Resource 7.1**, **Figure S7.3**. The dose was reduced in 13 subjects after they had either renal or hepatotoxicity or both.

The modelling analysis of renal toxicity showed that among the investigated baseline factors, the inclusion of age, sex, dose in mg/m^2, AUC_{base}, pC_{24h}, $pAUC_{24-\infty}$, or eGFR resulted in a significant decrease in OFV in the univariable covariate analysis, among which the baseline eGFR was the most significant predictor (ΔOFV = -52.8). The inclusion of toxicity status of the previous administration course did not result in a significant decrease in OFV. The treatment regimen itself was also not identified to affect the toxicity probability. The final model of renal toxicity included baseline eGFR (range: 40.2–158.7 mL/min/1.73m^2, maximum predicted probability change (maxΔP) = -0.929) and sex (for female, ΔP = -0.103) as significant covariates.

As for the hepatotoxicity model, AUC_{base}, dose in mg, and dose in mg/m^2 resulted in significant decreases in OFV in the univariable covariate analysis, among which dose

in mg/m^2 showed to be the most significant predictor (ΔOFV = -14.7). The inclusion of toxicity status of the previous administration cycle did not decrease OFV significantly. No additional covariates were significant after the inclusion of dose in mg/m^2, i.e. the final model of hepatotoxicity only included dose in mg/m^2 (range 1500–8000 mg/m^2, maxΔP = 0.86) as the most significant covariate.

The parameter estimates of the base and final toxicity models are shown in **Table 7.3**. The RSE of all parameters are < 40% indicating acceptable precision. The inclusion of covariates largely reduced the variance of the random IIV in both models. The VPC plots demonstrated an adequate model predictability for the probability of having renal toxicity, while the decreasing trend of hepatotoxicity over treatment courses was not well captured (**Online Resource 7.1**, **Figure S7.4**). The wider 90% prediction interval after the 4th administration cycle was due to the relatively small sample size at those cycles. **Figure 7.3** demonstrated the change of observed and predicted renal and hepatotoxicity probability as predictor values change. The simulation results showed that the median predicted probability of having renal toxicity decreased to less than 25% when baseline eGFR was higher than 66.6 mL/min/1.73m^2, and the median predicted probability of having hepatotoxicity increase to above 38.5% when dose raised above 3500 mg/m^2.

Table 7.3: Parameter estimates of the base and final logistic regression model of renal and hepatotoxicity

	Base model		Final model	
	Estimate	RSE (%) / [Shrinkage (%)]	Estimate	RSE (%) / [Shrinkage (%)]
Renal toxicity model				
θ	0.112	29%	0.0595	26%
θ_{eGFR}	-	-	-3.06	9%
θ_{SEX}			-1.32	32%
IIV (ω^2)	3.29	43% [35%]	1.11	61% [50%]
Hepatotoxicity model				
θ	0.289	11%	0.118	15%
θ_{DOSE}	-	-	2.25	38%
IIV (ω^2)	0.922	48% [41%]	0.708	52% [45%]

BSA, body surface area; IIV, inter-individual variability; RSE, relative standard error; eGFR, estimated glomerular filtration rate.

The exposure metrics C_{24h} and $AUC_{24-\infty}$ were identified to correlate with renal toxicity (ΔOFV = -75.3 and -85.6, respectively) in the univariable covariate analysis but not for hepatotoxicity. The parameter estimates can be found in **Online Resource 7.1**, **Table S7.2**. The observed proportion of patients with renal toxicity was 61% when C_{24h} > 8.64 µmol/L and 68.3% when $AUC_{24-\infty}$ > 109.5 µmol/L*h. According to the model simulations, the

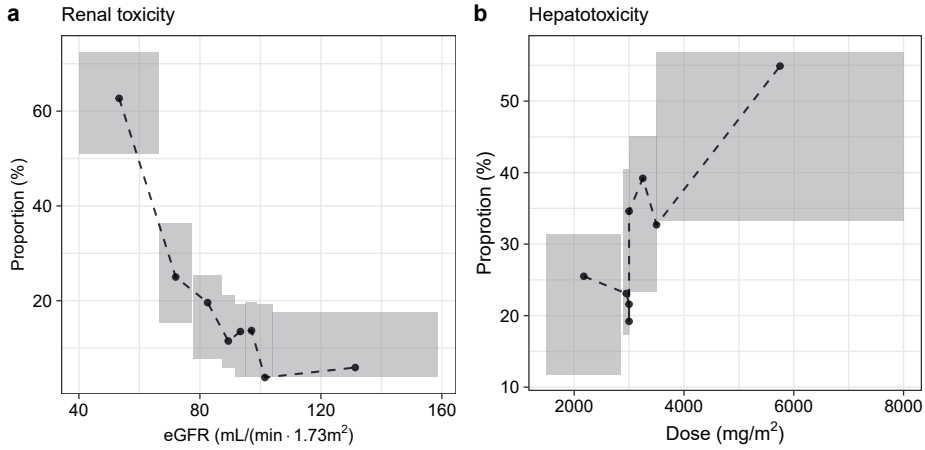

Figure 7.3: Visual predictive check of the model for renal toxicity probability over estimated glomerular filtration rate (eGFR) (a) and hepatotoxicity probability over dose (mg/m^2) (b). Black points represent the observations and shaded areas are the 90% prediction interval of the final models where binning was done based on the number of observations

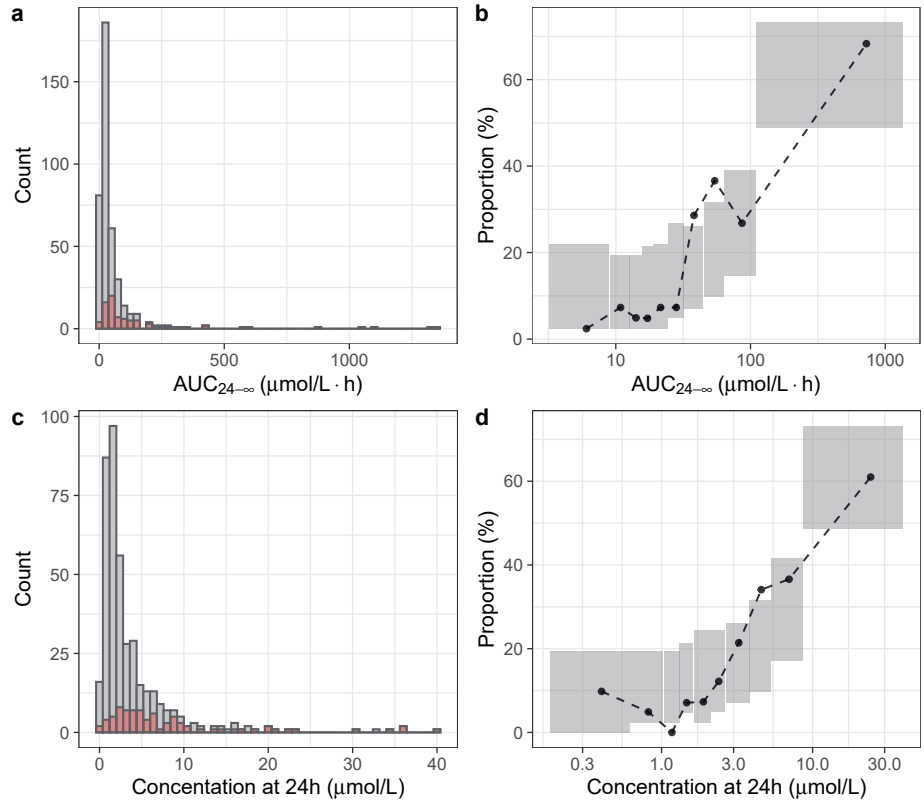

Figure 7.4: Distribution of (a) estimated $AUC_{24-\infty}$ and (c) simulated concentration at 24 hours (C_{24h}) of all treatment cycles (grey) and treatment cycles with renal toxicity (red), and observed and predicted probability of renal toxicity over (b) $AUC_{24-\infty}$ and (d) C_{24h}.

predicted median proportions of renal toxicity decreased from 61% to < 29.3% when C_{24h} decreased to ≤ 8.64 μmol/L, and from 61% to < 26.8% when $AUC_{24-\infty}$ decreased to ≤ 109.5 μmol/L*h, respectively. The distribution of estimated $AUC_{24-\infty}$ and C_{24h} of all treatment cycles and observed and predicted probability of renal toxicity over $AUC_{24-\infty}$ and C_{24h} were shown in **Figure 7.4**.

4. Discussion

In this study, a population PK model was developed for HD-MTX in patients with CNS lymphoma and covariates that explains HD-MTX PK variability were identified. Toxicity analysis identified baseline predictors for renal and hepatotoxicity, and the models allow to estimate the toxicity probability before each administration cycle. Additionally, potential exposure thresholds of $AUC_{24-\infty}$ and C_{24h} that indicate a high risk of renal toxicity were suggested to support better HD-MTX treatment.

The identified covariates on CL of MTX in the final model includes albumin and indicators of renal function, which are in accordance with the known PK characteristics of MTX [4, 5]. In addition, the CL of MTX also showed to vary among treatment regimens, which might suggest a need to alter the dose when targeting to the same level of exposure. The possible explanations for this finding could be the differences in infusion duration / rate of HD-MTX, patients' status, and the combined medications among these treatment groups. However, the impact of those factors cannot be distinguished as they highly overlapped with each other. A potential correlation between infusion duration/rate and MTX clearance has been mentioned previously. In those studies, higher CL or lower AUC has been observed in patients receiving HD-MTX with long infusion durations (24 hours) compared to short infusion durations (2–6 hours) [10, 28, 29]. In our study, high CL estimates under 24-hour infusion were also observed. In addition, a 4-hour infusion showed to correlate with low CL estimates compared with 1- or 3.25-hour infusion in our results (**Online Resource 7.1**, **Figure S7.2**). However, a clear physiological explanation for this observed phenomenon could not be found, and therefore dose alterations based on infusion duration specifically are not recommended.

Currently HD-MTX was dosed per BSA in CNS lymphoma patients. However, our study demonstrated that the influence of BSA on MTX PK is less significant than that of body weight, although these two factors are highly correlated and BSA has been identified as a covariate in previous PK studies [17, 20]. The estimated MTX $AUC_{24-\infty}$ and C_{24h} in our study population also showed an increasing trend over BSA (**Online Resource 7.1**, **Figure S7.5**). A few other studies have also pointed out that BSA is not the most predictive factor

to MTX PK, and BSA-guided dosing should be reconsidered especially for overweight patients [10, 30, 31]. Moreover, a dose reduction for HD-MTX has been suggested for patients with reduced renal function [7, 32]. Taking these facts into account, adjusting the MTX dose with the developed PK model which involves multiple covariates including renal function is considered to be more rational and accurate than BSA-guided dosing, and can help to further reduce PK variability.

The GOF plot of the final PK model showed that the population predictions underpredicted the lower concentrations (data points collected after 200 hours after last drug intake) while the individual predictions fitted well to the observations. These underpredicted concentrations all came from the treatment cycles where delayed elimination was observed. This suggests that the model structure could still be improved to better characterize the concentration-time curves in case of a delayed elimination. For example, an interaction between renal function and MTX PK, which may result in a time dependent MTX elimination, and non-linear elimination at low concentrations can be considered [33, 34]. A three-compartment model could also slightly better capture the delayed elimination. However, a reliable and stable three-compartment model could not be identified based on the current dataset. Since the individual fit of our model is considered to be adequate, a more complicated model was eventually not applied.

The toxicity analysis identified baseline predictors for HD-MTX-induced renal and hepatotoxicity which allow estimation of the toxicity probability before administration cycle. eGFR and sex were identified as significant baseline predictors for renal toxicity probability. Dose (mg/m^2) and age were also identified as significant predictors in the univariable analysis, which is consistent with previous findings [11, 13]. However, their influence did not remain significant after including eGFR in the model. Our findings suggest that to lower the probability of renal toxicity, the use of HD-MTX for patients with CNS lymphoma is recommended when eGFR > 66.6 mL/min/1.73m^2. This is in accordance with a previous review which indicated that renal function is a key prognostic factor for the tolerance of HD-MTX [32]. Accurately estimating the renal function of the patients before HD-MTX treatment may therefore be key in preventing toxicity during HD-MTX treatment. In patients with relatively low muscle mass, other eGFR measurement techniques such as a iohexol eGFR test could be applied [35]. Patients with a higher risk of toxicity that still need HD-MTX treatment should be carefully monitored and rescue therapy with high dose folate or in severe cases glucarpidase could be considered [36-38].

The dose of HD-MTX (mg/m^2) was identified to be the strongest predictor of hepatotoxicity. The results suggest that a high risk for hepatotoxicity in patients with CNS lymphoma is

foreseeable if the administrated dose of HD-MTX is higher than 3500 mg/m^2. In addition, the probability of hepatotoxicity appeared to decrease over treatment cycles which was not fully captured by the model. A possible explanation could be that patients tend to tolerate MTX better when treated for a longer period of time. Drop out due to toxicity is considered to be a less possible reason since less than 50% of subjects who stopped treatment after the first to third treatment courses had hepatotoxicity. Since the information on reason of drop out was not available, it was not considered in the analysis.

MTX exposure metrics was only identified to correlate with renal toxicity in patients with CNS lymphoma. To avoid the impact of possible inaccurate prediction of peak concentrations, $AUC_{24-\infty}$ was estimated and included in the analysis instead of $AUC_{0-\infty}$. We also investigated the correlation between C_{24h} and toxicity as a threshold on C_{24h} is valuable for early identification of patients at risk and early application of rescue treatment. Our results show that $AUC_{24-\infty}$ > 109.5 μmol/L*h or C_{24h} > 8.66 μmol/L correlate with high risk of renal toxicity in CNS lymphoma patients (> 60%). The threshold of C_{24h} is also in line with what was found in a previous study (10 μmol/L) [7].

Although high MTX exposure can result in toxicity, sufficient exposure is still essential to guarantee the efficacy. To better apply our findings to facilitate the individualization and optimization of HD-MTX therapy in patients with CNS lymphoma, an investigation on exposure-efficacy relationship is still needed. A previous study suggested that $AUC_{0-\infty}$ > 1100 μmol/L*h is associated with a favorable treatment outcome [12]. Due to an identified correlation of $AUC_{0-\infty}$ with C_{24h}, the same group recommend a C_{24h} target of 4–5 μmol/L [16]. Nonetheless, the direct relationship between C_{24h} or $AUC_{24-\infty}$ and the efficacy has not been reported. Thus, a further investigation on the relationship between C_{24h} or $AUC_{24-\infty}$ and efficacy would be beneficial to establish a therapeutic range for HD-MTX to support the individualization of HD-MTX dosage.

The current study has some limitations. First of all, due to the lack of data sampled in the first 12 hours after the start of MTX infusion, the developed model may not be able to well capture peak concentrations and provide a precise estimate of $AUC_{0-\infty}$. Nevertheless, our study demonstrated that $AUC_{24-\infty}$ and C_{24h} estimated with the model are also predictive to HD-MTX induced renal toxicity. Secondly, since this study was based on real-world data, the possibility of data not being recorded adequately enough may impact our analysis. Nevertheless, our findings may be more representative of real-world patients and are more translatable to clinical practice. Finally, although identified predictors have explained a large proportion of variability in HD-MTX induced toxicities, the unexplained variability remains large. Identifying covariates for the remained variability would be beneficial to

further improve the prediction. Previous studies have reported the influence of ABCC2 on PK of HD-MTX and the potential association of gene MTHFR, SLC19A1 and ABCB1 with MTX-induced hepatic toxicity [8, 21, 39]. Thus, the potential impact of pharmacogenetic polymorphisms would be of interest for future studies.

5. Conclusion

A population PK model was developed which adequately characterized the PK profile of HD-MTX in patients with CNS lymphoma. eGFR, treatment regimen, albumin, ALP, and body weight were identified as significant covariates that explain inter- and intra-individual variabilities in PK of HD-MTX. The toxicity analysis identified lower eGFR and male sex, and higher MTX dose (mg/m^2) as baseline predictors that are associated with higher risk of acute renal and hepatotoxicity, respectively. $AUC_{24-\infty}$ > 109.5 μmol/L*h and C_{24h} > 8.64 μmol/L were suggested to be potential exposure thresholds that predict a high risk of renal toxicity. These results hold a great potential for further individualizing HD-MTX dosage and preventing acute organ toxicity, which can improve HD-MTX therapy in CNS lymphoma patients.

Key points

- A population pharmacokinetic (PK) model was developed for high-dose methotrexate (HD-MTX) based on data collected from patients with central nervous system (CNS) lymphoma and subsequently used for exposure-toxicity analysis.
- Lower baseline eGFR and male sex are associated with increased risk of acute renal toxicity (grade ≥ 1). Higher MTX dose (mg/m^2) is associated with increased risk of acute hepatotoxicity (grade ≥ 1).
- The analysis identified that the MTX exposure metrics correlate with renal toxicity only, and area under the concentration-time curve from 24h to infinite ($AUC_{24-\infty}$) > 109.5 μmol/L*h and concentration at 24 hours (C_{24h}) > 8.64 μmol/L predicted a high risk of renal toxicity.

References

1. Fallah J, Qunaj L, Olszewski AJ. Therapy and outcomes of primary central nervous system lymphoma in the United States: analysis of the National Cancer Database. Blood Advances. 2016;1(2):112-21. doi:10.1182/bloodadvances.2016000927.
2. Calimeri T, Steffanoni S, Gagliardi F, Chiara A, Ferreri AJM. How we treat primary central nervous system lymphoma. ESMO Open. 2021;6(4):100213. doi:10.1016/j.esmoop.2021.100213.
3. Jeong SY, Yoon SE, Cho D, Kang ES, Cho J, Kim WS, et al. Real-world experiences of CNS-directed chemotherapy followed by autologous stem cell transplantation for secondary CNS involvement in relapsed or refractory diffuse large B-cell lymphoma. Front Oncol. 2022;12:1071281. doi:10.3389/fonc.2022.1071281.
4. Methotrexate Injection [package insert]. HOSPIRA. U.S. Food and Drug Administration. https://www.accessdata.fda.gov/drugsatfda_docs/label/2018/011719s125lbl.pdf. Revised April 2018. Accessed October 12, 2022.
5. Bannwarth B, Labat L, Moride Y, Schaeverbeke T. Methotrexate in Rheumatoid Arthritis. Drugs. 1994;47(1):25-50. doi:10.2165/00003495-199447010-00003.
6. Schmiegelow K. Advances in individual prediction of methotrexate toxicity: a review. Br J Haematol. 2009;146(5):489-503. doi:10.1111/j.1365-2141.2009.07765.x.
7. Howard SC, McCormick J, Pui C-H, Buddington RK, Harvey RD. Preventing and Managing Toxicities of High-Dose Methotrexate. The Oncologist. 2016;21(12):1471-82. doi:10.1634/theoncologist.2015-0164.
8. Benz-de Bretagne I, Zahr N, Le Gouge A, Hulot JS, Houillier C, Hoang-Xuan K, et al. Urinary coproporphyrin I/(I + III) ratio as a surrogate for MRP2 or other transporter activities involved in methotrexate clearance. Br J Clin Pharmacol. 2014;78(2):329-42. doi:10.1111/bcp.12326.
9. Kawakatsu S, Nikanjam M, Lin M, Le S, Saunders I, Kuo DJ, et al. Population pharmacokinetic analysis of high-dose methotrexate in pediatric and adult oncology patients. Cancer Chemother Pharmacol. 2019;84(6):1339-48. doi:10.1007/s00280-019-03966-4.
10. Ibarra M, Combs R, Taylor ZL, Ramsey LB, Mikkelsen T, Buddington RK, et al. Insights from a pharmacometric analysis of HDMTX in adults with cancer: Clinically relevant covariates for application in precision dosing. Br J Clin Pharmacol. 2022. doi:10.1111/bcp.15506.
11. Wight J, Ku M, Garwood M, Carradice D, Lasica M, Keamy L, et al. Toxicity associated with high-dose intravenous methotrexate for hematological malignancies. Leuk Lymphoma. 2022;63(10):2375-82. doi:10.1080/10428194.2022.2074987.
12. Joerger M, Huitema AD, Krähenbühl S, Schellens JH, Cerny T, Reni M, et al. Methotrexate area under the curve is an important outcome predictor in patients with primary CNS lymphoma: A pharmacokinetic-pharmacodynamic analysis from the IELSG no. 20 trial. British journal of cancer. 2010;102(4):673-7. doi:10.1038/sj.bjc.6605559.
13. Amitai I, Rozovski U, El-Saleh R, Shimony S, Shepshelovich D, Rozen-Zvi B, et al. Risk factors for high-dose methotrexate associated acute kidney injury in patients with hematological malignancies. Hematol Oncol. 2020;38(4):584-8. doi:10.1002/hon.2759.
14. Lalonde RL, Kowalski KG, Hutmacher MM, Ewy W, Nichols DJ, Milligan PA, et al. Model-based drug development. Clin Pharmacol Ther. 2007;82(1):21-32. doi:10.1038/sj.clpt.6100235.
15. Buil-Bruna N, Lopez-Picazo JM, Martin-Algarra S, Troconiz IF. Bringing Model-Based Prediction to Oncology Clinical Practice: A Review of Pharmacometrics Principles and Applications. Oncologist. 2016;21(2):220-32. doi:10.1634/theoncologist.2015-0322.

16. Joerger M, Ferreri AJ, Krähenbühl S, Schellens JH, Cerny T, Zucca E, et al. Dosing algorithm to target a predefined AUC in patients with primary central nervous system lymphoma receiving high dose methotrexate. Br J Clin Pharmacol. 2012;73(2):240-7. doi:10.1111/j.1365-2125.2011.04084.x.
17. Mei S, Li X, Jiang X, Yu K, Lin S, Zhao Z. Population Pharmacokinetics of High-Dose Methotrexate in Patients With Primary Central Nervous System Lymphoma. J Pharm Sci. 2018;107(5):1454-60. doi:10.1016/j.xphs.2018.01.004.
18. Blasco H, Senecal D, Le Gouge A, Pinard E, Benz-de Bretagne I, Colombat P, et al. Influence of methotrexate exposure on outcome in patients treated with MBVP chemotherapy for primary central nervous system lymphoma. Br J Clin Pharmacol. 2010;70(3):367-75. doi:10.1111/j.1365-2125.2010.03712.x.
19. Nader A, Zahran N, Alshammaa A, Altaweel H, Kassem N, Wilby KJ. Population Pharmacokinetics of Intravenous Methotrexate in Patients with Hematological Malignancies: Utilization of Routine Clinical Monitoring Parameters. Eur J Drug Metab Pharmacokinet. 2017;42(2):221-8. doi:10.1007/s13318-016-0338-1.
20. Arshad U, Taubert M, Seeger-Nukpezah T, Ullah S, Spindeldreier KC, Jaehde U, et al. Evaluation of body-surface-area adjusted dosing of high-dose methotrexate by population pharmacokinetics in a large cohort of cancer patients. BMC Cancer. 2021;21(1):719. doi:10.1186/s12885-021-08443-x.
21. Simon N, Marsot A, Villard E, Choquet S, Khe HX, Zahr N, et al. Impact of ABCC2 polymorphisms on high-dose methotrexate pharmacokinetics in patients with lymphoid malignancy. Pharmacogenomics J. 2013;13(6):507-13. doi:10.1038/tpj.2012.37.
22. ARK™ Methotrexate Assay [package insert]. ARK Diagnostics, Inc.. https://www.ark-tdm.com/products/cancer/methotrexate/pdfs/ARK_Methotrexate_Assay_Rev07_August_2017.pdf. Revised August 2017. Accessed June 05, 2020.
23. Levey AS, Stevens LA, Schmid CH, Zhang YL, Castro AF, 3rd, Feldman HI, et al. A new equation to estimate glomerular filtration rate. Ann Intern Med. 2009;150(9):604-12. doi:10.7326/0003-4819-150-9-200905050-00006.
24. Keizer RJ, Jansen RS, Rosing H, Thijssen B, Beijnen JH, Schellens JH, et al. Incorporation of concentration data below the limit of quantification in population pharmacokinetic analyses. Pharmacol Res Perspect. 2015;3(2):e00131. doi:10.1002/prp2.131.
25. Jonsson EN, Karlsson MO. Automated covariate model building within NONMEM. Pharm Res. 1998;15(9):1463-8. doi:10.1023/a:1011970125687.
26. NCI Common Terminology Criteria for Adverse Events (CTCAE) version 5.0. November 2017 [cited 2020 Octomber]; Available from: https://ctep.cancer.gov/protocoldevelopment/electronic_applications/docs/CTCAE_v5_Quick_Reference_5x7.pdf
27. Lindbom L, Pihlgren P, Jonsson EN. PsN-Toolkit--a collection of computer intensive statistical methods for non-linear mixed effect modeling using NONMEM. Comput Methods Programs Biomed. 2005;79(3):241-57. doi:10.1016/j.cmpb.2005.04.005.
28. Ferreri AJ, Guerra E, Regazzi M, Pasini F, Ambrosetti A, Pivnik A, et al. Area under the curve of methotrexate and creatinine clearance are outcome-determining factors in primary CNS lymphomas. British journal of cancer. 2004;90(2):353-8. doi:10.1038/sj.bjc.6601472.
29. Ramsey LB, Panetta JC, Smith C, Yang W, Fan Y, Winick NJ, et al. Genome-wide study of methotrexate clearance replicates SLCO1B1. Blood. 2013;121(6):898-904. doi:10.1182/blood-2012-08-452839.
30 Pai MP, Debacker KC, Derstine B, Sullivan J, Su GL, Wang SC. Comparison of Body Size, Morphomics, and Kidney Function as Covariates of High-Dose Methotrexate Clearance in Obese Adults with Primary Central Nervous System Lymphoma. Pharmacotherapy. 2020;40(4):308-19. doi:10.1002/phar.2379.

31. Gallais F, Oberic L, Faguer S, Tavitian S, Lafont T, Marsili S, et al. Body Surface Area Dosing of High-Dose Methotrexate Should Be Reconsidered, Particularly in Overweight, Adult Patients. Therapeutic Drug Monitoring. 2021;43(3):408-15. doi:10.1097/Ftd.0000000000000813.
32. Holdhoff M, Mrugala MM, Grommes C, Kaley TJ, Swinnen LJ, Perez-Heydrich C, et al. Challenges in the Treatment of Newly Diagnosed and Recurrent Primary Central Nervous System Lymphoma. J Natl Compr Canc Netw. 2020;18(11):1571-8. doi:10.6004/jnccn.2020.7667.
33. Woillard JB, Debord J, Benz-de-Bretagne I, Saint-Marcoux F, Turlure P, Girault S, et al. A Time-Dependent Model Describes Methotrexate Elimination and Supports Dynamic Modification of MRP2/ABCC2 Activity. Ther Drug Monit. 2017;39(2):145-56. doi:10.1097/ftd.0000000000000381.
34. Hendel J, Nyfors A. Nonlinear renal elimination kinetics of methotrexate due to saturation of renal tubular reabsorption. European Journal of Clinical Pharmacology. 1984;26(1):121-4. doi:10.1007/BF00546719.
35. Zwart TC, de Vries APJ, Engbers AGJ, Dam RE, van der Boog PJM, Swen JJ, et al. Model-Based Estimation of Iohexol Plasma Clearance for Pragmatic Renal Function Determination in the Renal Transplantation Setting. Clin Pharmacokinet. 2021;60(9):1201-15. doi:10.1007/s40262-021-00998-z.
36. Ramsey LB, Balis FM, O'Brien MM, Schmiegelow K, Pauley JL, Bleyer A, et al. Consensus Guideline for Use of Glucarpidase in Patients with High-Dose Methotrexate Induced Acute Kidney Injury and Delayed Methotrexate Clearance. Oncologist. 2018;23(1):52-61. doi:10.1634/theoncologist.2017-0243.
37. Schaff LR, Lobbous M, Carlow D, Schofield R, Gavrilovic IT, Miller AM, et al. Routine use of low-dose glucarpidase following high-dose methotrexate in adult patients with CNS lymphoma: an open-label, multi-center phase I study. BMC Cancer. 2022;22(1):60. doi:10.1186/s12885-021-09164-x.
38. Widemann BC, Balis FM, Kim A, Boron M, Jayaprakash N, Shalabi A, et al. Glucarpidase, leucovorin, and thymidine for high-dose methotrexate-induced renal dysfunction: clinical and pharmacologic factors affecting outcome. J Clin Oncol. 2010;28(25):3979-86. doi:10.1200/JCO.2009.25.4540.
39. Suthandiram S, Gan GG, Zain SM, Bee PC, Lian LH, Chang KM, et al. Effect of polymorphisms within methotrexate pathway genes on methotrexate toxicity and plasma levels in adults with hematological malignancies. Pharmacogenomics. 2014;15(11):1479-94. doi:10.2217/pgs.14.97.

Online Resource 7.1: Supplementary figures and tables

Supplementary Figures

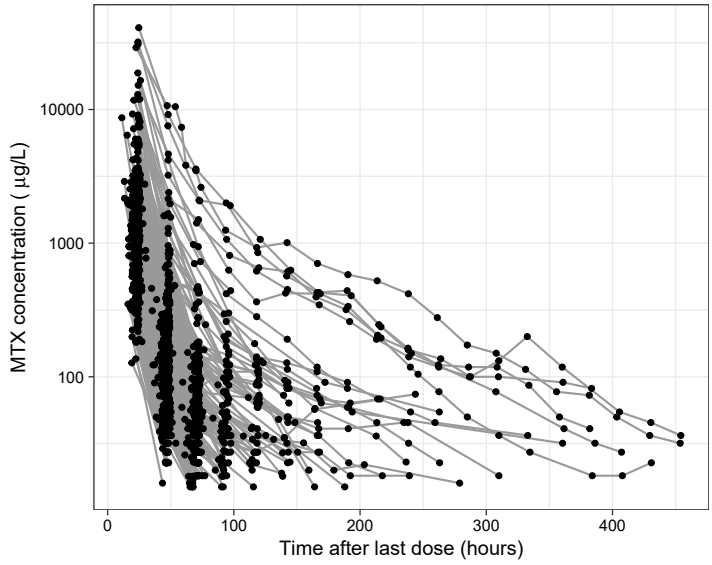

Figure S7.1: The collected methotrexate concentration-time curves in patients with CNS lymphoma on semi-logarithmic scale (n = 110 patients).

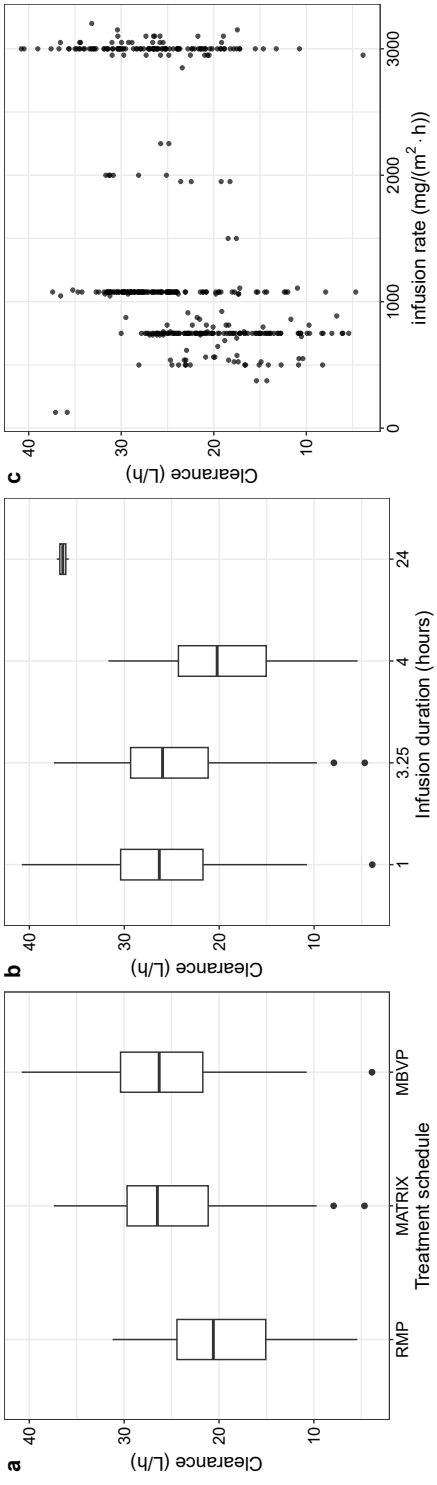

Figure S7.2: Estimated MTX clearance versus (a) treatment regimen, (b) infusion duration (hours), and (c) infusion rate.

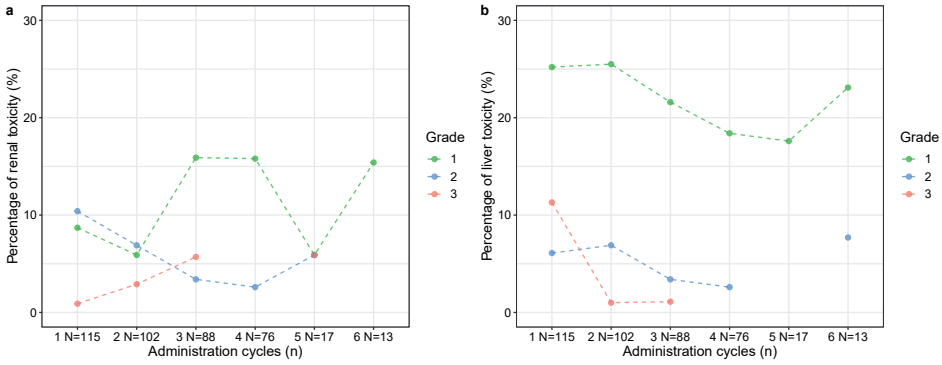

Figure S7.3: Observed percentage of renal (a) and liver (b) toxicity under each treatment cycle separated by the toxicity grade.

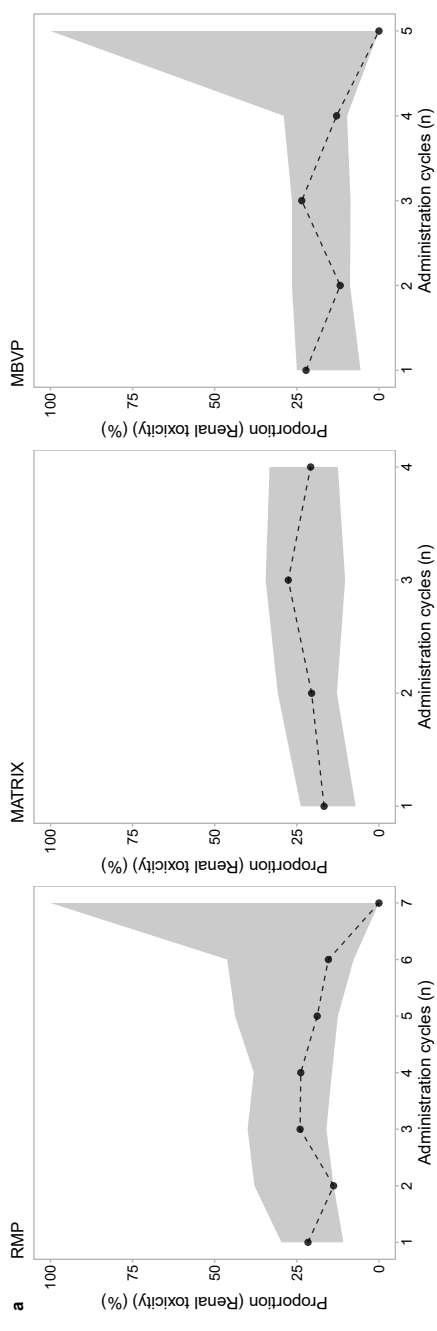

Figure S7.4: Visual predictive check of model for renal toxicity probability (a) and hepatotoxicity probability (b) by treatment regimens. Black points represent the observations and shaded areas are the 90% prediction interval of the final model.

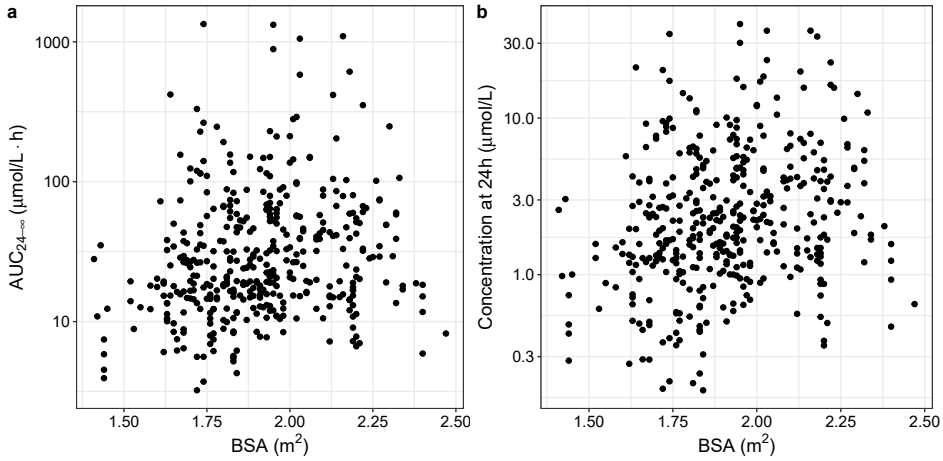

Figure S7.5: Estimated area under the concentration-time curve between 24 hours after drug administration to infinity ($AUC_{24-\infty}$) (a) and concentration at 24 hours (b) versus body surface area of the included patients.

Supplementary Tables

Table S7.1: Characteristics of the HD-MTX treatment regimens of the included patients

	N of administrations (%) / Median (Range)		
Treatment regimen	RMP	MATRIX	MBVP
Age of patients (years)	72 (28–83)	58.5 (22–67)	66 (51–76)
Infusion duration			
a. 4 hours	133 (93.7%)	6 (4.5%)	0
b. 14–25% dose 15 mins, and the rest 3 hours	9 (6.3%)	126 (94.0%)	0
c. 10% dose 1 hour, and the rest 23 hours	0	2 (1.5%)	0
d. 1 hour	0	0	136 (100%)
Infusion rate (mg/m^2/h)	750 (375–1077)	1076 (125–2000)	3000 (1500–3200)
Dose of MTX (mg/m^2)	3000 (1500–3650)	3500 (1750–8000)	3000 (1500–3200)
Dose intensity (days)	14.0 (12.9–54.1)	23.0 (11.0–66.9)	15.0 (6–45)
Co-medications	rituximab and procarbazine	high-dose cytarabine, thiotepa, and rituximab	teniposide, carmustine, prednisolone with/without rituximab or high dose cytarabine

Table S7.2: Parameter estimates of the logistic regression model of renal toxicity with exposure metrics included as predictors

	Estimate	RSE (%) / [Shrinkage (%)]
Renal toxicity model with $AUC_{24-\infty}$		
θ	0.0135	61%
$\theta_{AUC_{24-\infty}}$	0.746	11%
IIV (ω^2)	5.69	55% [38%]
Renal toxicity model with C_{24h}		
θ	0.0132	64%
$\theta_{C_{24h}}$	0.851	10%
IIV (ω^2)	6.04	55% [37%]

IIV, inter-individual variability; RSE, relative standard error; $AUC_{24-\infty}$, area under the concentration-time curve between 24 hours after drug administration to infinity; C_{24h}, MTX concentration at 24 hours after drug administration.